INTERNATIONAL JOURNAL FOR NUMERICAL METHODS IN FLUIDS
Int. J. Numer. Meth. Fluids 2007; **55**:347–366
Published online 14 March 2007 in Wiley InterScience (www.interscience.wiley.com). DOI: 10.1002/fld.1464

Optimal flow control for Navier–Stokes equations: Drag minimization

L. Dedè*, †

MOX—Modeling and Scientific Computing, *Dipartimento di Matematica*, *Politecnico di Milano*, *via Bonardi 9*, *I-20133*, *Milano*, *Italy*

SUMMARY

Optimal control and shape optimization techniques have an increasing role in Fluid Dynamics problems governed by partial differential equations (PDEs). In this paper, we consider the problem of drag minimization for a body in relative motion in a fluid by controlling the velocity through the body boundary. With this aim, we handle with an optimal control approach applied to the steady incompressible Navier–Stokes equations. We use the Lagrangian functional approach and we consider the Lagrangian multiplier method for the treatment of the Dirichlet boundary conditions, which include the control function itself. Moreover, we express the drag coefficient, which is the functional to be minimized, through the variational form of the Navier–Stokes equations. In this way, we can derive, in a straightforward manner, the adjoint and sensitivity equations associated with the optimal control problem, even in the presence of Dirichlet control functions. The problem is solved numerically by an iterative optimization procedure applied to state and adjoint PDEs which we approximate by the finite element method. Copyright © 2007 John Wiley & Sons, Ltd.

Received 27 June 2006; Revised 22 January 2007; Accepted 22 January 2007

KEY WORDS: optimal control problems; Navier–Stokes equations; drag minimization; Dirichlet boundary control; Lagrangian multiplier method; finite element approximation

1. INTRODUCTION

A popular problem in Fluid Dynamics consists in minimizing the drag coefficient of a body in relative motion with a fluid [1–9]; in particular, one case commonly studied is that of the steady incompressible Navier–Stokes equations with constant density and viscosity. Some applications are, e.g. the design of airfoils in Aerodynamics [8] (at high Reynolds numbers) and the study of the

*Correspondence to: L. Dedè, MOX—Modeling and Scientific Computing, Dipartimento di Matematica, Politecnico di Milano, *via* Bonardi 9, I-20133, Milano, Italy.
†E-mail: luca.dede@polimi.it

Contract/grant sponsor: Publishing Arts Research Counsil; contract/grant number: 98-1846389

geometry of blunt bodies in flows at low Reynolds numbers (see, e.g. [10]). The drag minimization problem can be recast in the theory of optimal control for partial differential equations (PDEs) [11, 12], or as a problem of shape optimization [4, 9]. In this paper, we are interested in minimizing the drag coefficient of a blunt body by acting on the velocity at the boundaries of the body itself; this corresponds to regulate the aspiration or the blowing of the boundary layer in order to reduce the effects of the vortices coming off from the rear of the body. This problem can be formulated as an optimal control problem, for which the control function is the Dirichlet boundary condition [2, 3, 5–7, 13–15]. With this aim, we use the Lagrangian functional approach [1, 5, 16–18] instead of calculating directly the gradient of the functional subject to minimization [2, 3, 5, 7, 14]. In this context, the main difficulty consists in the treatment of the Dirichlet boundary control function, which does not match with the variational setting provided by the Lagrangian functional approach, unless suitable lifting terms are introduced.

Different approaches have been considered in the literature to overcome this difficulty in the field of Navier–Stokes equations. In [13], the Nitsche method [19] is proposed in order to suppress the recirculation in a backward facing step in a channel by regulating the inflow velocity field. In [15, 20], both linear and non-linear penalized Neumann control approaches for the solution of optimal control problems with the Dirichlet control functions are considered. Moreover, in [15], a Lagrangian multiplier method [21] is proposed for the treatment of the Dirichlet control function (this strategy is also considered in [22] for optimal control problems governed by elliptic PDEs). The approaches presented in [15, 20] are applied for the minimization of the vorticity and the 'distance' between the velocity field and a desired one; sequential quadratic programming (SQP) methods (see, e.g. [23]) have been used for the solution of these optimal control problems.

In this paper, we use, for our drag minimization problem, the Lagrangian multiplier method for the treatment of the Dirichlet velocity control function on the body, in analogy with the approaches outlined in [15, 22] (for elliptic PDEs). However, for the evaluation of the drag, or more in general the force acting on the body, we exploit the variational form of the Navier–Stokes equations [24], instead of using the definition, the latter being directly related to the integral of the stress acting on the body boundaries. The two approaches, that are equivalent at the 'continuous level', are in fact different at the 'discrete level'. The one that we follow in this paper yields more accurate computation of the drag coefficient [24] and, in the context of optimization, reduces the propagation of the discretization errors in the course of the iterative optimization procedure. Moreover, this approach allows us to identify the Lagrangian multiplier as the inward directed normal stress, to express the drag coefficient in terms of this multiplier and, consequently, to obtain a simple expression for the adjoint equations.

For the numerical solution of the optimal control problem, we use the steepest-descent method [11], while the PDE system is discretized by means of the finite element (FE) method. Finally, we report some numerical results concerning with the minimization of the drag for blunt bodies (at low Reynolds numbers), which prove the effectiveness of the outlined procedures.

An outline of this work is as follows. In Section 2, we recall the Lagrangian functional approach for optimal control problems in an abstract setting. Then, we consider the drag coefficient minimization problem for the incompressible Navier–Stokes equations, introducing the evaluation of the drag coefficient by means of the variational form. Finally, we write the Lagrangian functional, using the Lagrangian multiplier method for the treatment of the Dirichlet boundary conditions, and we formulate the adjoint Navier–Stokes equations and the sensitivity equation. In Section 3, we discuss the aspects related to the numerical resolution of the optimal control problem: in particular, we recall the steepest-descent method and the techniques considered for the numerical solution of

DOI: 10.1002/fld

the Stokes and Navier–Stokes equations. Finally, in Section 4, we present some numerical results and compare them for different values of the Reynolds number.

2. MATHEMATICAL MODEL: THE OPTIMAL CONTROL PROBLEM

In this section, we consider the optimal control problem in an abstract setting; then, we treat a flow control problem governed by the Navier–Stokes equations for the minimization of the drag acting on a solid object.

2.1. The general setting for optimal control

Let us start with an abstract control problem, which, for the sake of simplicity, we consider depending on scalar variables; however, this formalism can be extended in straightforward manner to vectorial problems, like the Navier–Stokes equations which we will consider in Section 2.3.

The optimal control problem reads:

$$\text{find } u \in \mathscr{U},\ u = \operatorname{argmin} J(v,u) \text{ with } A(v) = f + B(u) \text{ and } v \in \mathscr{V} \tag{1}$$

where $J(v,u)$ is the *cost functional*, A a differential operator on $\mathscr{V}$ with values in $\mathscr{V}'$, B a differential operator on $\mathscr{U}$ into $\mathscr{V}'$, f a source term, $\mathscr{V}$ and $\mathscr{U}$ two Hilbert spaces. The equation $A(v) = f + B(u)$, which incorporates appropriate boundary conditions, is called the *state equation*, v the state variable and u the *control* variable. Let us note that, in general, $A(\cdot)$ and $B(\cdot)$ are non-linear differential operators in v and u, respectively.

For the analysis of the optimal control problem (1), we use the *Lagrangian functional* framework [1, 16–18]. This approach sets the control problem as a constrained minimization problem, for which a Lagrangian functional is defined; the minimum, if it exists, is a stationary 'point' of the Lagrangian functional. Conversely, the classical approach developed by Lions [12] allows a full analysis of the problem, providing existence and uniqueness results; incidentally, this technique is not always straightforward as the Lagrangian functional one, which, however, does not always provide a suitable analysis of the optimal control problem.

We define the Lagrangian functional as [16]

$$\mathscr{L}(v,z,u) := J(v,u) +_{\mathscr{V}} \langle z,\ f + B(u) - A(v)\rangle_{\mathscr{V}'} \tag{2}$$

where $z \in \mathscr{V}$ is the Lagrangian multiplier. The optimum of the control problem $\mathbf{x}^* := (v^*, z^*, u^*) \in \mathscr{X}$ ($\mathscr{X} := \mathscr{V} \times \mathscr{V} \times \mathscr{U}$), if it exists, is a stationary point of the Lagrangian functional $\mathscr{L}(\mathbf{x})$, with $\mathbf{x} := (v,z,u) \in \mathscr{X}$, i.e.

$$\nabla \mathscr{L}(\mathbf{x}^*)[\mathbf{y}] = \mathbf{0}, \quad \mathbf{y} \in \mathscr{X} \tag{3}$$

where differentiation is in Fréchet sense [25]. System (3) is regarded as the Euler–Lagrange system, for which we have the following three equations:

$$\begin{aligned} &\mathscr{L}_{,v}(v,z,u)[\vartheta] = 0 \quad \text{adjoint equation} \\ &\mathscr{L}_{,z}(v,z,u)[\phi] = 0 \quad \text{state equation} \\ &\mathscr{L}_{,u}(v,z,u)[\psi] = 0 \quad \text{'sensitivity' equation} \end{aligned} \tag{4}$$

DOI: 10.1002/fld

where we have supposed $\mathbf{y} = (\vartheta, \phi, \psi)$. The first equation of system (4) is regarded as the *adjoint equation*, for which $z \in \mathscr{V}$ is defined as the adjoint variable. The third equation is related to the sensitivity of the Lagrangian functional $\mathscr{L}(v, z, u)$ w.r.t. the control variable $u \in \mathscr{U}$.

Let us apply the general expression for the Lagrangian functional (3) to the abstract control problem stated in Equation (1); to this aim, we consider the weak form of the state equation, given in Equation (1) in distributional sense, which reads

$$\text{find } v \in \mathscr{V} : a(v)(\phi) = (f, \phi) + b(u)(\phi) \quad \forall \phi \in \mathscr{V} \tag{5}$$

where $a(\cdot)(\cdot)$ and $b(\cdot)(\cdot)$ are the semi-linear forms (linear in the second argument) associated, respectively, to the operators $A(\cdot)$ and $B(\cdot)$. The Lagrangian functional (2) reads

$$\mathscr{L}(v, z, u) = J(v, u) + (f, z) + b(u)(z) - a(v)(z) \tag{6}$$

By differentiating $\mathscr{L}(v, p, u)$ w.r.t. $v \in \mathscr{V}$, we obtain the adjoint equation in weak form:

$$\text{find } z \in \mathscr{V} : a'(v)(z, \vartheta) = J_{,v}(v, u)(\vartheta) \quad \forall \vartheta \in \mathscr{V} \tag{7}$$

where, for the sake of simplicity, we indicate $a_{,v}(v)(z, \vartheta)$ as $a'(v)(z, \vartheta)$; let us note that the adjoint equation is linear in $z \in \mathscr{V}$ even if the state equation is non-linear in the state variable. Similarly, by differentiating w.r.t. $u \in \mathscr{U}$ the third equation of the Euler–Lagrange system (4), we obtain

$$J_{,u}(v, u)(\psi) + b'(u)(z, \psi) = 0, \quad \psi \in \mathscr{U} \tag{8}$$

where we indicate $b_{,u}(u)(z, \psi)$ with $b'(u)(z, \psi)$. From the previous equation, it is possible to extract the sensitivity function $\delta u \in \mathscr{U}$, which we will define in Section 2.3 for the problem under investigation.

2.2. Drag minimization for Navier–Stokes equations

We consider a body embedded in a 2-D flow governed by the steady incompressible Navier–Stokes equations for a Newtonian fluid with constant density and viscosity.

The goal consists in minimizing the drag coefficient by regulating the flow $\mathbf{u}$ across the boundary Γ_{CTRL} of the body in relative steady motion with the fluid; see Figure 1. By defining $\mathbf{v}$ as the velocity field, p as the pressure, μ as dynamic viscosity coefficient, ρ as the density, the Navier–Stokes system reads [19, 26]

$$\begin{aligned}
&-\nabla \cdot \mathbb{T}(\mathbf{v}, p) + \rho(\mathbf{v} \cdot \nabla)\mathbf{v} = \mathbf{0} && \text{in } \Omega \\
&\nabla \cdot \mathbf{v} = 0 && \text{in } \Omega \\
&\mathbf{v} = \mathbf{v}_\infty && \text{on } \Gamma_{\text{IN}} \\
&\mathbf{v} \cdot \hat{\mathbf{n}} = 0, \quad (\mathbb{T}(\mathbf{v}, p)\hat{\mathbf{n}}) \cdot \hat{\mathbf{t}} = 0 && \text{on } \Gamma_{\text{SYM}} \\
&\mathbb{T}(\mathbf{v}, p)\hat{\mathbf{n}} = \mathbf{0} && \text{on } \Gamma_{\text{OUT}} \\
&\mathbf{v} = \mathbf{0} && \text{on } \Gamma_{\text{NS}} \\
&\mathbf{v} = \mathbf{u} && \text{on } \Gamma_{\text{CTRL}}
\end{aligned} \tag{9}$$

DOI: 10.1002/fld

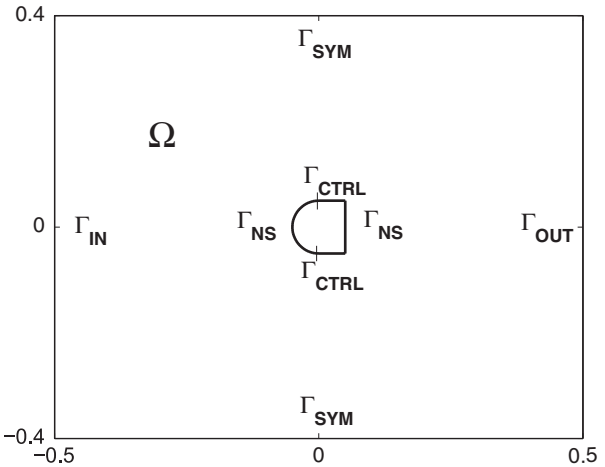

Figure 1. Domain for the control problem and boundary conditions.

where $\hat{\mathbf{n}}$ and $\hat{\mathbf{t}}$ are, respectively, the outward directed normal and tangential unit vectors on the boundary Γ_i; the *stress tensor* $\mathbb{T}(\mathbf{v}, p)$ reads

$$\mathbb{T}(\mathbf{v}, p) = \mu(\nabla\mathbf{v} + \nabla^{\mathrm{T}}\mathbf{v}) - p\mathbb{I} \tag{10}$$

$\mathbb{I}$ being the identity tensor. We impose inflow boundary conditions on Γ_{IN}, symmetry conditions on Γ_{SYM}, no stress conditions on Γ_{OUT}, no slip conditions on Γ_{NS} and Dirichlet conditions ($\mathbf{u}$ is the control variable) on the control boundary Γ_{CTRL}, which corresponds to imposing the velocity on Γ_{CTRL}. Let us note that $\bigcup_i \Gamma_i = \partial\Omega$ and $\Gamma_i \cap \Gamma_j = \emptyset, \forall i, j$.

The functional to minimize is the adimensional drag coefficient $c_{\mathrm{D}}(\mathbf{v}, p)$, for which the problem that we consider is

$$\text{find } \mathbf{u} = \text{ argmin } c_{\mathrm{D}}(\mathbf{v}, p) \quad \text{with } c_{\mathrm{D}}(\mathbf{v}, p) := -\frac{1}{q_\infty d}\oint_{\Gamma_{\mathrm{BODY}}} (\mathbb{T}(\mathbf{v}, p)\hat{\mathbf{n}}) \cdot \hat{\mathbf{v}}_\infty \, \mathrm{d}\Gamma \tag{11}$$

and $(\mathbf{v}, p)$ depends on $\mathbf{u}$ through the state equations (9). The minus sign takes into account that, by convention, the force is positive if acting on the fluid. In Equation (11) $\Gamma_{\mathrm{BODY}} := \Gamma_{\mathrm{NS}} \cup \Gamma_{\mathrm{CTRL}}$, $q_\infty := \frac{1}{2}\rho V_\infty^2$, with $\mathbf{v}_\infty = V_\infty \hat{\mathbf{v}}_\infty$, $\hat{\mathbf{v}}_\infty$ is the unit vector directed as the incoming flow, V_∞ is taken constant and d is the characteristic dimension of the body. Let us note that the drag $q_\infty d c_{\mathrm{D}}$ has the dimension of a force per unit length.

We consider a parabolic profile for the control flow, written in the form

$$\mathbf{u} = U\mathbf{g}(\mathbf{x}) \quad \text{with } \mathbf{g}(\mathbf{x}) := -4\frac{(\mathrm{x} - \mathrm{x1}_{\mathrm{CTRL}})(\mathrm{x2}_{\mathrm{CTRL}} - \mathrm{x})}{(\mathrm{x2}_{\mathrm{CTRL}} - \mathrm{x1}_{\mathrm{CTRL}})^2}\hat{\mathbf{n}}_{\mathrm{CTRL}} \tag{12}$$

where $\mathrm{x1}_{\mathrm{CTRL}}$ and $\mathrm{x2}_{\mathrm{CTRL}}$ are the abscissae of the endpoints of the boundary Γ_{CTRL}, while $\hat{\mathbf{n}}_{\mathrm{CTRL}}$ is the outward directed unit vector normal to Γ_{CTRL}. Let us note that the *versus* of the unit vector $\hat{\mathbf{n}}_{\mathrm{CTRL}}$ is from the fluid towards the body, which is external to the computational domain; moreover, on Γ_{CTRL}, we have $\mathbf{g}(\mathrm{x}) \cdot \hat{\mathbf{n}}_{\mathrm{CTRL}} \leqslant 0$. The effective control variable is the parameter $U \in \mathbb{R}$, which is the maximum value (in modulus) of the parabolic flow of Equation (12). Let us observe that

DOI: 10.1002/fld

a positive value of U corresponds to a blowing of the fluid across the body walls Γ_{CTRL}; on the contrary, if U is negative, the fluid is aspirated (i.e. the flow is directed from the fluid towards the body).

Weak formulation: For the analysis of the optimal control problem we introduce, similar to what was done in Section 2.1 for the general case, the weak form of the Navier–Stokes equations. This can be done by introducing suitable functional spaces for $\mathbf{v}$ and p [19, 26], which account properly for Dirichlet boundary conditions; an alternative approach consists in introducing the boundary conditions by means of a Lagrange multiplier approach [15, 21, 22]. This last approach, which we will follow, allows a straightforward treatment of the boundary conditions in the analysis of the optimal control problem, without introducing lifting terms.

Let us introduce the following forms:

$$a(\mathbf{v}, \mathbf{\Phi}) := \int_\Omega \mu(\nabla \mathbf{v} + \nabla^{\mathrm{T}} \mathbf{v}) \cdot \nabla \mathbf{\Phi} \, \mathrm{d}\Omega \tag{13}$$

$$b(p, \mathbf{\Phi}) := -\int_\Omega p \nabla \cdot \mathbf{\Phi} \, \mathrm{d}\Omega \tag{14}$$

$$c(\mathbf{v}, \mathbf{v}, \mathbf{\Phi}) := \int_\Omega \rho(\mathbf{v} \cdot \nabla)\mathbf{v} \cdot \mathbf{\Phi} \, \mathrm{d}\Omega \tag{15}$$

The Navier–Stokes equations in weak form, with boundary conditions introduced through a Lagrange multiplier, read

$$\begin{gathered}
\text{find } \mathbf{v} \in [H^1(\Omega)]^2, \quad p \in L^2(\Omega), \quad \mathbf{w} \in [H^{-1/2}(\Gamma_{\mathrm{DS}})]^2 : \\
a(\mathbf{v}, \mathbf{\Phi}) + b(p, \mathbf{\Phi}) + c(\mathbf{v}, \mathbf{v}, \mathbf{\Phi}) + \int_{\Gamma_{\mathrm{D}}} \mathbf{w} \cdot \mathbf{\Phi} \, \mathrm{d}\Gamma + \int_{\Gamma_{\mathrm{SYM}}} \mathbf{w} \cdot \hat{\mathbf{n}} \, \mathbf{\Phi} \cdot \hat{\mathbf{n}} \, \mathrm{d}\Gamma = 0 \\
b(\varphi, \mathbf{v}) = 0 \\
\int_{\Gamma_{\mathrm{D}}} (\mathbf{v} - \mathbf{v}_{\mathrm{D}}) \cdot \mathbf{\Lambda} \, \mathrm{d}\Gamma + \int_{\Gamma_{\mathrm{SYM}}} \mathbf{v} \cdot \hat{\mathbf{n}} \mathbf{\Lambda} \cdot \hat{\mathbf{n}} \, \mathrm{d}\Gamma = 0 \\
\forall \mathbf{\Phi} \in [H^1(\Omega)]^2 \quad \forall \varphi \in L^2(\Omega) \quad \forall \mathbf{\Lambda} \in [H^{-1/2}(\Gamma_{\mathrm{DS}})]^2
\end{gathered} \tag{16}$$

where $\Gamma_{\mathrm{D}} := \Gamma_{\mathrm{IN}} \cup \Gamma_{\mathrm{NS}} \cup \Gamma_{\mathrm{CTRL}}$, $\Gamma_{\mathrm{DS}} := \Gamma_{\mathrm{D}} \cup \Gamma_{\mathrm{SYM}}$, $[H^1(\Omega)]^2$ and $[H^{-1/2}(\Gamma_{\mathrm{DS}})]^2$ are the usual Sobolev spaces, while $\mathbf{v}_{\mathrm{D}}$, which we consider in the Sobolev space $[H^{1/2}(\Gamma_{\mathrm{D}})]^2$, reads (Equation (9))

$$\mathbf{v}_{\mathrm{D}} := \begin{cases} \mathbf{v}_\infty & \text{on } \Gamma_{\mathrm{IN}} \\ \mathbf{0} & \text{on } \Gamma_{\mathrm{NS}} \\ \mathbf{u} & \text{on } \Gamma_{\mathrm{CTRL}} \end{cases} \tag{17}$$

In particular, the control variable $\mathbf{u} \in [H^{1/2}(\Gamma_{\mathrm{CTRL}})]^2$. The Lagrange multiplier $\mathbf{w} \in [H^{-1/2}(\Gamma_{\mathrm{DS}})]^2$ is introduced to allow the variable $\mathbf{v} \in [H^1(\Omega)]^2$ to fit the Dirichlet boundary conditions, which includes the control variable $\mathbf{u}$. Let us observe that we suppose $\hat{\mathbf{n}}$ (i.e. Γ_{SYM}) to be 'sufficiently regular' so that in Equation (16) $\mathbf{w} \in [H^{-1/2}(\Gamma_{\mathrm{SYM}})]^2$ implies $\mathbf{w} \cdot \hat{\mathbf{n}} \in H^{-1/2}(\Gamma_{\mathrm{SYM}})$, $\mathbf{v} \in [H^{1/2}(\Gamma_{\mathrm{SYM}})]^2$ implies $\mathbf{v} \cdot \hat{\mathbf{n}} \in H^{1/2}(\Gamma_{\mathrm{SYM}})$, and so on. This is the case of the problem under investigation

DOI: 10.1002/fld

(see Figure 1), for which Γ_{SYM} is composed by two distinct segments. Moreover, the boundary integrals of Equation (16) can be seen as duality pairs: ${}_{H^{-1/2}(\Gamma_i)}\langle\cdot,\cdot\rangle_{H^{1/2}(\Gamma_i)}$ or ${}_{H^{1/2}(\Gamma_i)}\langle\cdot,\cdot\rangle_{H^{-1/2}(\Gamma_i)}$. Finally, in view of the finite element approximation, problem (16) will be reformulated in weak form [19]; the solution $\tilde{\mathbf{v}}$ is sought for in $[H^1_{|\Gamma_{\mathrm{DS}}}(\Omega)]^2$, the test function $\mathbf{\Phi}\in[H^1_{|\Gamma_{\mathrm{DS}}}(\Omega)]^2$, where $[H^1_{|\Gamma_{\mathrm{DS}}}(\Omega)]^2:=\{\mathbf{s}\in[H^1(\Omega)]^2:\ \mathbf{s}_{|\Gamma_{\mathrm{D}}}=\mathbf{0}$ and $(\mathbf{s}\cdot\hat{\mathbf{n}})_{|\Gamma_{\mathrm{SYM}}}=0\}$, by modifying the source term in order to account for the non-homogeneous Dirichlet data. Thereby the direct evaluation of the variable $\mathbf{w}\in[H^{-1/2}(\Gamma_{\mathrm{DS}})]^2$ is not necessary.

Drag evaluation: The drag coefficient c_{D}, defined in Equation (11), can be evaluated once the Navier–Stokes equations are resolved and the velocity field $\mathbf{v}$ and the pressure p are known. However, the computation of c_{D} by means of the definition (11) can lead to inaccurate results even if the computational grid is quite fine, as we better specify later. Better results can be achieved by using an alternative expression for c_{D}, which we indicate with $\tilde{c}_{\mathrm{D}}$, dependent on the variational forms used for the Navier–Stokes equations, as reported in [7, 17, 24].

In order to provide the expression of $\tilde{c}_{\mathrm{D}}$, we express c_{D} (11) in the following form

$$c_{\mathrm{D}}(\mathbf{v},p)=\frac{1}{q_\infty d}\oint_{\partial\Omega}(\mathbb{T}(\mathbf{v},p)\hat{\mathbf{n}})\cdot\mathbf{\Phi}_\infty\,\mathrm{d}\Gamma \tag{18}$$

where

$$\mathbf{\Phi}_\infty\in[H^1(\Omega)]^2\quad\text{with }\mathbf{\Phi}_{\infty|\Gamma_{\mathrm{BODY}}}=-\hat{\mathbf{v}}_\infty,\quad \mathbf{\Phi}_{\infty|\partial\Omega\setminus\Gamma_{\mathrm{BODY}}}=\mathbf{0} \tag{19}$$

By means of the Gauss theorem and Green's identity [24, 26], Equation (18) becomes

$$\begin{aligned}c_{\mathrm{D}}(\mathbf{v},p)&=\frac{1}{q_\infty d}\int_\Omega\nabla\cdot(\mathbb{T}(\mathbf{v},p)^{\mathrm{T}}\mathbf{\Phi}_\infty)\,\mathrm{d}\Omega\\&=\frac{1}{q_\infty d}\int_\Omega(\nabla\cdot\mathbb{T}(\mathbf{v},p)\cdot\mathbf{\Phi}_\infty+\mathbb{T}(\mathbf{v},p)\cdot\nabla\mathbf{\Phi}_\infty)\,\mathrm{d}\Omega\end{aligned} \tag{20}$$

Owing to the first equation of the system (9) and Equation (15), we have

$$\int_\Omega\nabla\cdot\mathbb{T}(\mathbf{v},p)\cdot\mathbf{\Phi}_\infty\,\mathrm{d}\Omega=\int_\Omega\rho(\mathbf{v}\cdot\nabla)\mathbf{v}\cdot\mathbf{\Phi}_\infty\,\mathrm{d}\Omega=c(\mathbf{v},\mathbf{v},\mathbf{\Phi}_\infty) \tag{21}$$

while, from Equations (10), (13) and (14), we obtain

$$\begin{aligned}\int_\Omega\mathbb{T}(\mathbf{v},p)\cdot\nabla\mathbf{\Phi}_\infty\,\mathrm{d}\Omega&=\int_\Omega\mu(\nabla\mathbf{v}+\nabla^{\mathrm{T}}\mathbf{v})\cdot\nabla\mathbf{\Phi}_\infty\,\mathrm{d}\Omega-\int_\Omega p\nabla\cdot\mathbf{\Phi}_\infty\,\mathrm{d}\Omega\\&=a(\mathbf{v},\mathbf{\Phi}_\infty)+b(p,\mathbf{\Phi}_\infty)\end{aligned} \tag{22}$$

for which, being $b(\varphi,\mathbf{v})=0$, $\forall\varphi\in L^2(\Omega)$, $\tilde{c}_{\mathrm{D}}$ reads

$$\tilde{c}_{\mathrm{D}}(\mathbf{v},p)=\frac{1}{q_\infty d}\mathscr{A}(\mathbf{v},p,\mathbf{\Phi}_\infty,\varphi)\quad\forall\varphi\in L^2(\Omega) \tag{23}$$

where

$$\mathscr{A}(\mathbf{v},p,\mathbf{\Phi},\varphi):=a(\mathbf{v},\mathbf{\Phi})+b(p,\mathbf{\Phi})+b(\varphi,\mathbf{v})+c(\mathbf{v},\mathbf{v},\mathbf{\Phi}) \tag{24}$$

DOI: 10.1002/fld

The form for the drag coefficient provided in Equation (23) allows accurate computations and will be used in this work. Let us note that c_D and $\tilde{c}_D$ are equivalent at the continuous level, however, the representations (20) and (23) lead to different approximations at the discrete level. For instance, by using the FE method with continuous, piecewise polynomials of degree k for $\mathbf{v}$ and $k-1$ for p (Taylor–Hood elements, see [19, 27, 28]), the order of convergence of $\tilde{c}_{Dh}$ to the exact value c_D is $2k$, while for c_{Dh} is only k [24], being c_{Dh} and $\tilde{c}_{Dh}$ the computed quantities corresponding to c_D and $\tilde{c}_D$. This fact has great importance in the optimization context, where the adjoint variables depend on the sensitivity of the cost functional (in this case c_D) with respect to the state variables. The choice of the representation, as verified by numerical tests, not only influences the computation of the adjoint variables, but it also affects the accuracy of the result obtained by the optimization procedure.

Let us observe that, according to Equation (16), the variational form $\mathscr{A}(\mathbf{v}, p, \mathbf{\Phi}, \varphi)$ can be expressed as

$$\mathscr{A}(\mathbf{v}, p, \mathbf{\Phi}, \varphi) = -\int_{\Gamma_D} \mathbf{w}\cdot\mathbf{\Phi}\,d\Gamma - \int_{\Gamma_{SYM}} \mathbf{w}\cdot\hat{\mathbf{n}}\mathbf{\Phi}\cdot\hat{\mathbf{n}}\,d\Gamma \tag{25}$$

for which, upon the definition of $\mathbf{\Phi}_\infty$ given in Equation (19), the drag coefficient $\tilde{c}_D$ admits the alternative expression:

$$\hat{c}_D(\mathbf{w}) = \frac{1}{q_\infty d}\int_{\Gamma_{BODY}} \mathbf{w}\cdot\hat{\mathbf{v}}_\infty\,d\Gamma \tag{26}$$

Let us note that Equation (26) allows us to identify the Lagrange multiplier $\mathbf{w}\in[H^{-1/2}(\Gamma_{DS})]^2$ as the inward normal stress, more precisely

$$\mathbf{w} = -\mathbb{T}(\mathbf{v}, p)\hat{\mathbf{n}} \quad \text{on } \Gamma_{DS} \tag{27}$$

This last result allows us to derive in a straightforward manner the adjoint equations associated to the control problem, as we will show in the following section.

2.3. The optimal control system for the Navier–Stokes equations

We apply the optimal control analysis based on the Lagrangian functional given in Section 2.1 to the drag minimization problem defined in Equation (11).

According to Equations (16), (24) and (26), the associated Lagrangian functional is defined as

$$\begin{aligned}\mathscr{L}(\mathbf{v}, p, \mathbf{w}, \mathbf{z}, q, \mathbf{r}, \mathbf{u}) := \hat{c}_D(\mathbf{w}) - \mathscr{A}(\mathbf{v}, p, \mathbf{z}, q)\\ -\int_{\Gamma_D} \mathbf{w}\cdot\mathbf{z}\,d\Gamma - \int_{\Gamma_{SYM}} \mathbf{w}\cdot\hat{\mathbf{n}}\mathbf{z}\cdot\hat{\mathbf{n}}\,d\Gamma\\ -\int_{\Gamma_D\setminus\Gamma_{CTRL}} (\mathbf{v}-\mathbf{v}_D)\cdot\mathbf{r}\,d\Gamma - \int_{\Gamma_{CTRL}} (\mathbf{v}-\mathbf{u})\cdot\mathbf{r}\,d\Gamma\\ -\int_{\Gamma_{SYM}} \mathbf{v}\cdot\hat{\mathbf{n}}\mathbf{r}\cdot\hat{\mathbf{n}}\,d\Gamma\end{aligned} \tag{28}$$

DOI: 10.1002/fld

By differentiating $\mathscr{L}(\cdot)$ with respect to $(\mathbf{z}, q, \mathbf{r})$, we obtain the state equation in weak form reported in Equation (16). Similarly, by differentiating $\mathscr{L}(\cdot)$ with respect to the state variables $(\mathbf{v}, p, \mathbf{w})$, we obtain the adjoint equations. Their weak form reads

$$\text{find } \mathbf{z}\in[H^1(\Omega)]^2, \quad q\in L^2(\Omega), \quad \mathbf{r}\in[H^{-1/2}(\Gamma_{\mathrm{DS}})]^2:$$

$$a(\boldsymbol{\Theta}, \mathbf{z}) + b(q, \boldsymbol{\Theta}) + c'(\mathbf{v}, \boldsymbol{\Theta}, \mathbf{z}) + \int_{\Gamma_{\mathrm{D}}} \boldsymbol{\Theta}\cdot\mathbf{r}\,\mathrm{d}\Gamma + \int_{\Gamma_{\mathrm{SYM}}} \boldsymbol{\Theta}\cdot\hat{\mathbf{n}}\mathbf{r}\cdot\hat{\mathbf{n}}\,\mathrm{d}\Gamma = 0$$

$$b(\vartheta, \mathbf{z}) = 0$$

$$\int_{\Gamma_{\mathrm{D}}} \boldsymbol{\Upsilon}\cdot\mathbf{z}\,\mathrm{d}\Gamma + \int_{\Gamma_{\mathrm{SYM}}} \boldsymbol{\Upsilon}\cdot\hat{\mathbf{n}}\mathbf{z}\cdot\hat{\mathbf{n}}\,\mathrm{d}\Gamma = \hat{c}_{\mathrm{D}}(\boldsymbol{\Upsilon}) \tag{29}$$

$$\forall\boldsymbol{\Theta}\in[H^1(\Omega)]^2 \quad \forall\vartheta\in L^2(\Omega) \quad \forall\boldsymbol{\Upsilon}\in[H^{-1/2}(\Gamma_{\mathrm{DS}})]^2$$

where, according to Equation (15)

$$c'(\mathbf{v}, \boldsymbol{\Theta}, \mathbf{z}) := c(\boldsymbol{\Theta}, \mathbf{v}, \mathbf{z}) + c(\mathbf{v}, \boldsymbol{\Theta}, \mathbf{z}) \tag{30}$$

This adjoint problem corresponds to the linearized Navier–Stokes equations (Oseen equations) around $\mathbf{v}$ with the following boundary conditions

$$\begin{aligned}
&\mathbf{z} = \mathbf{0} && \text{on } \Gamma_{\mathrm{IN}}\\
&\mathbf{z} = \hat{\mathbf{v}}_\infty/(q_\infty d) && \text{on } \Gamma_{\mathrm{BODY}}\\
&\mathbf{z}\cdot\hat{\mathbf{n}} = 0, \quad (\mathbb{T}(\mathbf{z}, q)\hat{\mathbf{n}})\cdot\hat{\mathbf{t}} = 0 && \text{on } \Gamma_{\mathrm{SYM}}\\
&\mathbb{T}(\mathbf{z}, q)\hat{\mathbf{n}} = \mathbf{0} && \text{on } \Gamma_{\mathrm{OUT}}
\end{aligned} \tag{31}$$

Finally, by differentiating $\mathscr{L}(\cdot)$ with respect to the control variable $\mathbf{u}$, we have

$$\int_{\Gamma_{\mathrm{CTRL}}} \boldsymbol{\Psi}\cdot\mathbf{r}\,\mathrm{d}\Gamma = 0 \quad \forall\boldsymbol{\Psi}\in[H^{1/2}(\Gamma_{\mathrm{CTRL}})]^2 \tag{32}$$

After considering the form (12) for $\mathbf{u}$, the previous equation reads

$$\int_{\Gamma_{\mathrm{CTRL}}} \psi\mathbf{g}(\mathbf{x})\cdot\mathbf{r}\,\mathrm{d}\Gamma = 0 \quad \forall\psi\in\mathbb{R} \tag{33}$$

The sensitivity δU can be written in the following form

$$\delta U = \int_{\Gamma_{\mathrm{CTRL}}} \mathbf{g}(\mathbf{x})\cdot\mathbf{r}\,\mathrm{d}\Gamma \tag{34}$$

which is identically equal to zero at the optimum. Let us note that the sensitivity δU depends on the adjoint stress $\mathbf{r}$; by similar arguments to those considered for the computation of the drag

DOI: 10.1002/fld

coefficient and by manipulating Equation (29), Equation (34) equivalently reads

$$\delta U = -\mathscr{A}'(\mathbf{G}, \vartheta, \mathbf{z}, q, \mathbf{v}) \quad \forall \vartheta \in L^2(\Omega) \tag{35}$$

where

$$\mathscr{A}'(\mathbf{\Theta}, \vartheta, \mathbf{z}, q, \mathbf{v}) := a(\mathbf{\Theta}, \mathbf{z}) + b(q, \mathbf{\Theta}) + b(\vartheta, \mathbf{z}) + c'(\mathbf{\Theta}, \mathbf{v}, \mathbf{z}) \tag{36}$$

being

$$\mathbf{G} \in [H^1(\Omega)]^2 \quad \text{with } \mathbf{G}_{|\Gamma_{\text{CTRL}}} = \mathbf{g}(\mathbf{x}), \quad \mathbf{G}_{|\partial\Omega \setminus \Gamma_{\text{CTRL}}} = \mathbf{0} \tag{37}$$

3. NUMERICAL DISCRETIZATION

To solve the optimal control problem, we consider the Galerkin-FE method for the numerical solution of the state and adjoint equations (Navier–Stokes and Oseen type) and an iterative approach for functional minimization.

3.1. The optimization iterative method

We describe, by referring to the abstract framework of Section 2.1, the optimization method considered for the solution of the optimal control problem.

The optimum of the control problem (1) is the solution of the Euler–Lagrange system (3) (or (4)), which is composed by the state, adjoint and 'sensitivity' equations. The system is, in general, fully coupled, in the sense that each equation involves all the variables (v, z, u), with the exception of the state equation which does not depend on the adjoint variable z. The solution of the control problem can be obtained by solving the complete system (3); however, the computational cost associated with this method could be very large.

An alternative approach, which we consider in this work, is based on the following iterative optimization procedure, which involves the steepest-descent method (see [11, 29]):

1. start with an initial control variable u^0;
2. solve the state equation/s, from which we obtain v^j;
3. compute the value of the cost functional $J(v^j, u^j)$;
4. solve the adjoint equation/s, given the control variable and once the state variables are computed (we obtain z^j);
5. extract the sensitivity δu^j from the third equation of the Euler–Lagrange system (Equation (8));
6. compute the norm of the sensitivity $\|\delta u^j\|_{\mathscr{U}}$;
7. compare the norm of the sensitivity with a stopping criterium tolerance Tol_{IT}:
   - if $\|\delta u^j\|_{\mathscr{U}} \geqslant \text{Tol}_{\text{IT}}$, perform an iterative step on the control variable:
   $$u^{j+1} = u^j - \tau^j \delta u^j \tag{38}$$
   and return to point 2;
   - if $\|\delta u^j\|_{\mathscr{U}} < \text{Tol}_{\text{IT}}$, stop.

The relaxation parameter τ^j can be chosen on the basis of the optimal control properties [11, 29].

DOI: 10.1002/fld

Let us notice that for the optimal control problem under investigation, according to Equation (35), the norm of sensitivity reads

$$\|\delta u\|_{\mathscr{U}} = |\delta U| = |\mathscr{A}'(\mathbf{G}, \vartheta, \mathbf{z}, q, \mathbf{v})| \quad \forall \vartheta \in L^2(\Omega) \tag{39}$$

where $\mathbf{G}$ is chosen according to Equation (36).

3.2. *Numerical solution of state and adjoint equations*

Both the state and adjoint equations enforce the Dirichlet boundary conditions in weak form, by means of Lagrangian multipliers, through the state and adjoint stresses $\mathbf{w}$ and $\mathbf{r}$. However, for the numerical solution, we can re-write these equations in a conventional manner introducing appropriate functional spaces and lifting terms. In this way, we omit to compute explicitly the state and adjoint stresses $\mathbf{w}$ and $\mathbf{r}$.

The state equations consist of the steady Navier–Stokes equations, while the adjoint ones correspond to a steady Oseen problem. In fact, the adjoint equations are linear in both the adjoint variables (velocity and pressure), being the term $c'(\mathbf{v}, \boldsymbol{\Theta}, \mathbf{z})$ (30) linear w.r.t. the adjoint velocity $\mathbf{z}$. Let us note that the adjoint equations depend on the state variables uniquely through the term $c'(\mathbf{v}, \boldsymbol{\Theta}, \mathbf{z})$; for this reason, the FE matrix corresponding to this term needs to be recomputed at each step of the optimization iterative procedure.

First, we recall briefly a method for the solution of the Stokes equations, which is employed to solve the adjoint equations and to initialize the state Navier–Stokes equations. Then, we consider the Newton method, with Uzawa preconditioning for the solution of the Navier–Stokes equations. Other and more efficient numerical methods for the solution of Stokes and Navier–Stokes equations, both steady and time dependent, can be used (see, e.g. [19, 26, 30–32]).

Solution of steady Stokes equations: In order to satisfy the inf–sup (LBB) condition [19], we consider the $\mathbb{P}^2$–$\mathbb{P}^1$ continuous FE pair for the velocity and the pressure, respectively (for both state and adjoint ones). By considering a generic Stokes problem (see, e.g. Equation (9) without the non-linear term) the corresponding discretized problem reads

$$\begin{aligned} A\mathbf{V} + B^{\mathrm{T}}\mathbf{P} &= \mathbf{F} \\ B\mathbf{V} &= \mathbf{0} \end{aligned} \tag{40}$$

where the matrices A and B corresponds to the variational forms $a(\cdot,\cdot)$ and $b(\cdot,\cdot)$, respectively (Equations (13) and (14)), $\mathbf{F}$ is the source term vector (including the lifting terms), while $\mathbf{V}$ and $\mathbf{P}$ are, respectively, the vectors of the unknown FE coefficients for the velocity and pressure. The problem is resolved by computing firstly the pressure vector $\mathbf{P}$ and then the velocity $\mathbf{V}$ vector:

$$BA^{-1}B^{\mathrm{T}}\mathbf{P} = BA^{-1}\mathbf{F} \tag{41}$$

$$A\mathbf{V} = \mathbf{F} - B^{\mathrm{T}}\mathbf{P} \tag{42}$$

Both systems admit unique solution, being the matrix A symmetric and positive definite and the rank of B maximum (due to the FE pair considered), that can be obtained by means of the conjugate gradient (CG) method [33], being the matrix $BA^{-1}B^{\mathrm{T}}$ symmetric and positive definite.

DOI: 10.1002/fld

Remark 3.1
In the case of the Oseen problem for the adjoint equation, the matrix A arises from the variational forms $a(\cdot,\cdot)$ and $c'(\cdot,\cdot,\cdot)$ (Equations (13) and (30)), for which A is no longer symmetric; in this case for the solution of the linear systems (41) and (42) the GMRES method [33] has been considered.

Solution of steady Navier–Stokes equations: The Navier–Stokes equations for an incompressible fluid with constant properties can be seen as a compact perturbation of the Stokes equations, with the addition of a non-linear term in the velocity variable. The system can be solved by means of the Newton method, solving at each step of the iterative procedure an Oseen problem, which arises by linearizing the Navier–Stokes equations. These linearized equations at the generic step $k+1$, obtained from Equation (9), read

$$\begin{aligned} -\nabla\cdot\mathbb{T}(\mathbf{v}^{(k+1)},p^{(k+1)})+\mathbf{c}'(\mathbf{v}^{(k)},\mathbf{v}^{(k+1)})+\mathbf{c}'(\mathbf{v}^{(k+1)},\mathbf{v}^{(k)}) &= \mathbf{c}'(\mathbf{v}^{(k)},\mathbf{v}^{(k)}) && \text{in } \Omega \\ \nabla\cdot\mathbf{v}^{(k+1)} &= 0 && \text{in } \Omega \\ \text{B.C.s} && && \text{on } \partial\Omega \end{aligned} \tag{43}$$

where $\mathbf{v}^{(k)}$ is the velocity computed at the previous iterative step and $\mathbf{c}'(\cdot,\cdot)$ is defined as

$$\mathbf{c}'(\mathbf{r},\mathbf{q}):=\rho(\mathbf{r}\cdot\nabla)\mathbf{q} \tag{44}$$

The Newton algorithm reads:

1. solve the Stokes problem, computing the initial pressure and velocity field;
2. by considering the velocity computed at the previous step $\mathbf{v}^{(k)}$, solve the Oseen problem, corresponding to Equation (43), obtaining $\mathbf{v}^{(k+1)}$ and $p^{(k+1)}$.
3. compute the appropriate norms of the incremental differences $\mathbf{v}^{(k+1)}-\mathbf{v}^{(k)}$ and $p^{(k+1)}-p^{(k)}$ and compare them with a prescribed tolerance;
4. if the stopping criterium is fulfilled, take $\mathbf{v}^{(k+1)}$ and $p^{(k+1)}$ as solutions of the Navier–Stokes equations; otherwise, set $\mathbf{v}^{(k)}=\mathbf{v}^{(k+1)}$, $p^{(k)}=p^{(k+1)}$ and return to point 2.

A preconditioning matrix can be used for the solution of the linear system (41) corresponding to the Stokes (or Oseen) equations, which are recursively solved in the Newton method. In particular, we consider the Uzawa preconditioning matrix D, which corresponds to the bilinear form $d(p,q):=\int_\Omega pq\,\mathrm{d}\Omega$.

No stabilization terms for convection are used in the discrete Navier–Stokes equations, as we are interested in flows at low Reynolds numbers (inferior to 50) and we suppose to handle with sufficiently refined meshes. Moreover, as previously mentioned, a divergence-stable FE pair is considered, so that stabilization terms for the pressure do not need to be used.

Remark 3.2
At each step of the optimization iterative procedure, we solve the Navier–Stokes state equations, for which an initialization by means of a Stokes problem occurs. In order to save computational costs, we can take as initial guess the state velocity computed at the previous step of the optimization procedure, instead of computing it by means of a Stokes problem solver. The validity of this procedure is confirmed by numerical tests (see Section 4).

Other techniques for the reduction of the computational cost of the optimization procedure can be considered, such as, e.g. reduced order methods (see [5, 6]).

DOI: 10.1002/fld

4. NUMERICAL RESULTS

We present some numerical results concerning the drag minimization control problem outlined in Section 2, carried out by means of the FE library *FreeFEM++* [34].

In particular, referring to Equations (9) and (11) and Figure 2, we chose $\rho = 1$, $V_\infty = 1$ and $d = 0.1$ (body length), for which, defining the Reynolds number:

$$Re := \frac{\rho V_\infty d}{\mu} \tag{45}$$

the dynamic viscosity coefficient μ can be deduced. At the initial step of the optimization procedure, we initialize $\mathbf{u} = \mathbf{0}$, for which, according to Equation (12), $U = 0$ and $U_{\text{av}} = \frac{2}{3}U = 0$, U_{av} being the average value of $\mathbf{u}$ on Γ_{CTRL}. We take the relaxation parameter $\tau^j = \tau = 0.5$ (Equation (38)) and we consider a tolerance $\text{Tol}_{\text{IT}} = 1/1000|\delta U^0|$ for the stopping criterium of the optimization method outlined in Section 3.1, where the superscript 0 means at the initial step and δU is reported in Equation (39). Moreover, we provide the computing times (cpu times) required for the solution of the optimal control problems; the computations have been carried out on an AMD Athlon 1.8 GHz processor, with 256 KB of memory cache and 1 GB of RAM.

Test 1: Referring to Figure 2, we consider the case for which $t = d = 0.1$. For the computations we use the mesh reported in Figure 3 with 2955 triangular elements (and 1565 vertices); in the sequel, we provide also a comparison of the results for three different meshes.

Firstly, we consider the case for which $Re = 10$. In Figure 4, we report the velocity field and pressure, solution of the state Navier–Stokes equations, obtained for $U_{\text{av}} = 0$; in Figure 5, the streamlines for the state velocity field are presented. In Figure 6, we show the adjoint velocity and pressure, computed at the initial step of the optimization iterative procedure (corresponding to $U_{\text{av}} = 0$). At the end of the optimization procedure, we obtain the velocity field and the pressure reported in Figure 7; in Figure 8, the streamlines of the optimal velocity field show the effects of the optimization. In particular, the initial drag coefficient $c_{\text{D}} = 3.8332$, corresponding to $U_{\text{av}} = 0$, is reduced, by means of this procedure, to the optimal one, which is $c_{\text{D}} = 3.3066$, obtained for $U_{\text{av}} = -0.96676$ (this corresponds to an aspiration of the flow across the control boundaries of

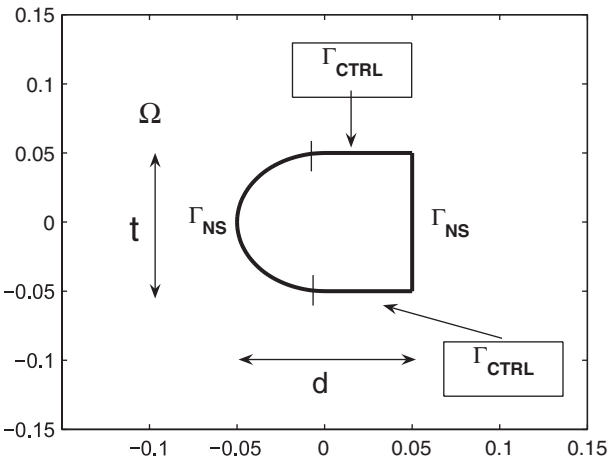

Figure 2. Zoom around the body, geometry and boundary conditions.

DOI: 10.1002/fld

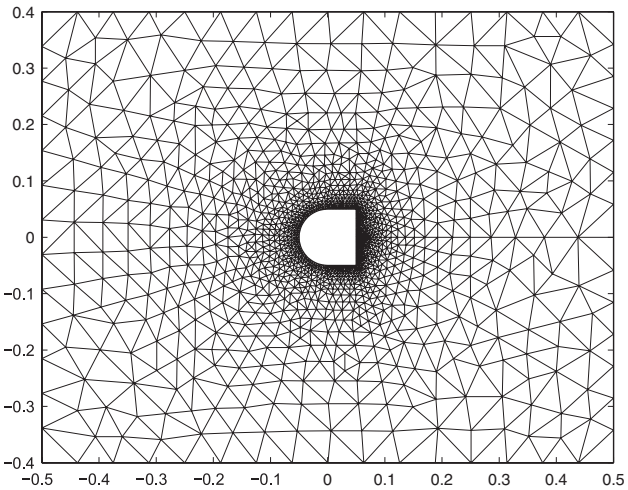

Figure 3. Test 1: mesh with 2955 elements.

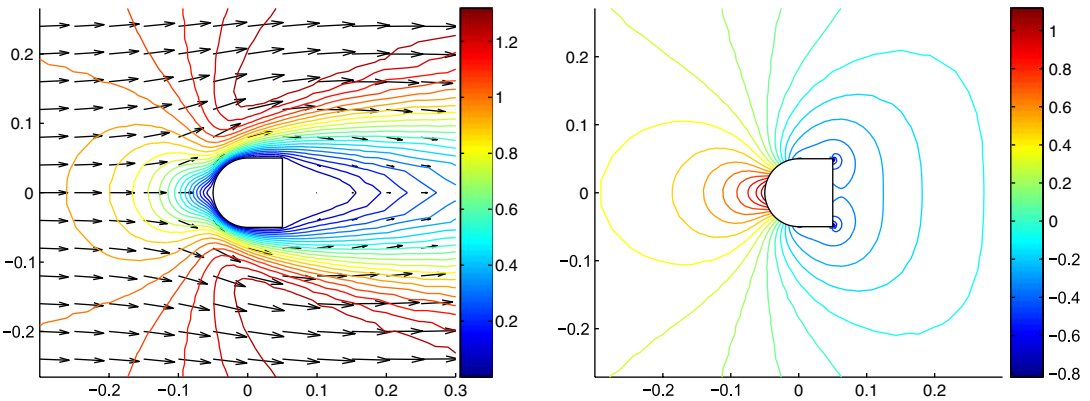

Figure 4. Test 1: zoom of velocity field (left) and pressure (right) for the initial state flow ($Re = 10$).

the body). In Figure 9, we report the behaviour of the drag coefficient c_D and the sensitivity $|\delta U|$ (normalized w.r.t. $|\delta U^0|$) *versus* the number of iterations of the optimization procedure, for which the convergence occurs in 24 iterations. Let us observe that the convergence of c_D to the optimal value is quick; e.g. after $j = 11$ optimization steps, we have that $|\delta U^j|/|\delta U^0| < \frac{1}{50}$ and the relative percent errors on c_D and U_{av} (optimal), computed w.r.t. the optimal quantities, are, respectively, 0.03 and 3.8%. In Figure 10, we show the values of c_D obtained by solving the Navier–Stokes state equations for different values of U_{av}; this confirms that the local minimum value of c_D corresponds to that obtained by means of the optimization procedure, for which $U_{av} = -0.96676$.

In Table I, we report the values of c_D (with $U_{av} = 0$) for different Reynolds numbers Re, the corresponding optimal drag coefficients, the optimal control functions U_{av}, the number of iterations of the optimization procedure and the corresponding cpu time. In particular, we find that, when Re increases, the modulus of the optimal U_{av} decreases, as the number of iterations of the optimization

DOI: 10.1002/fld

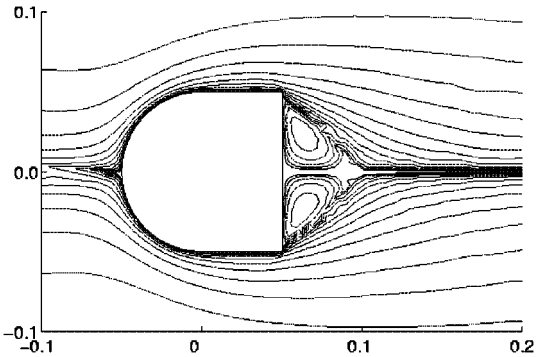

Figure 5. Test 1: streamlines for the initial state flow (zoom) ($Re = 10$).

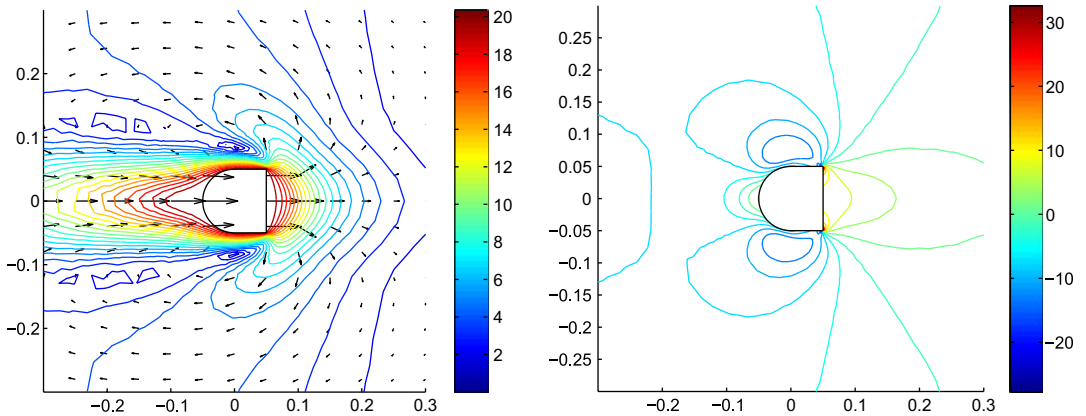

Figure 6. Test 1: zoom of adjoint velocity field (left) and adjoint pressure (right) for the initial adjoint flow ($Re = 10$).

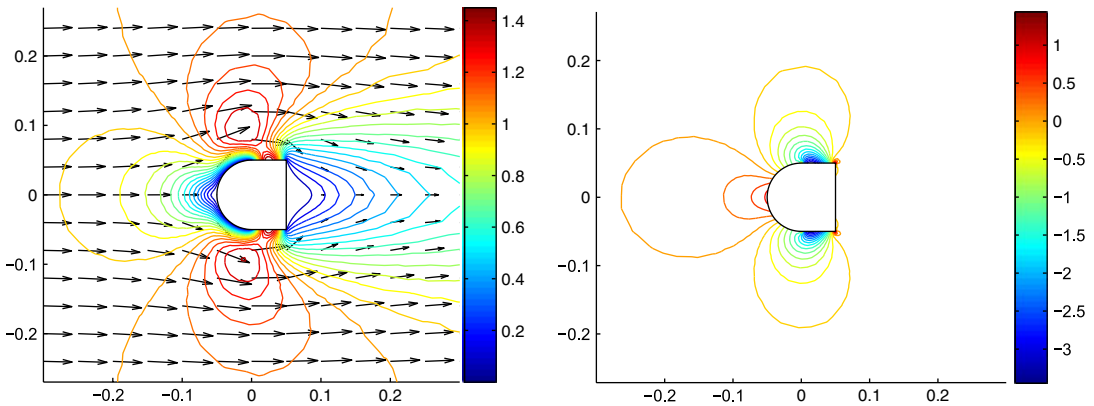

Figure 7. Test 1: zoom of velocity field (left) and pressure (right) for the optimal state flow ($Re = 10$).

DOI: 10.1002/fld

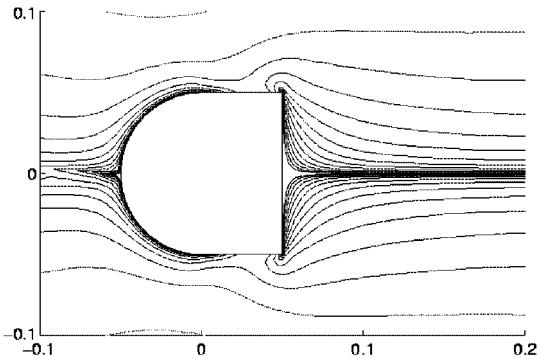

Figure 8. Test 1: streamlines for the optimal state flow ($Re = 10$).

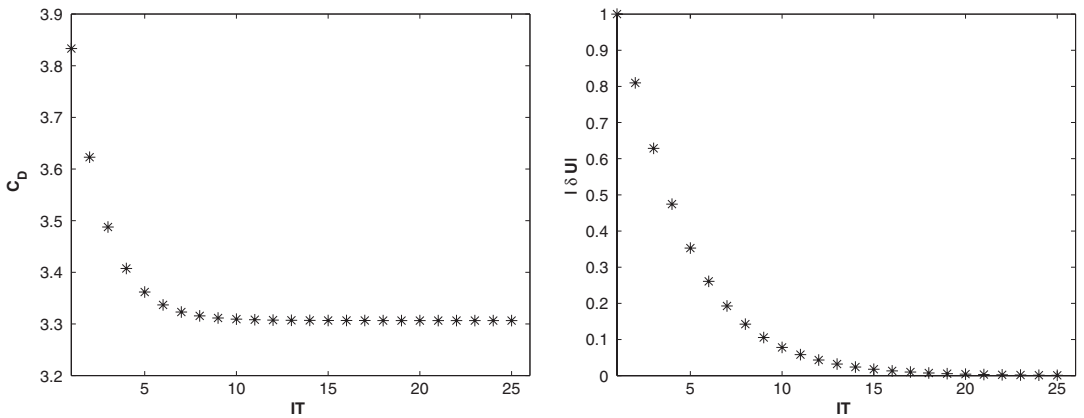

Figure 9. Test 1: drag coefficient (left) and sensitivity (right), normalized with δU^0, *versus* number of iterations of the optimization procedure ($Re = 10$).

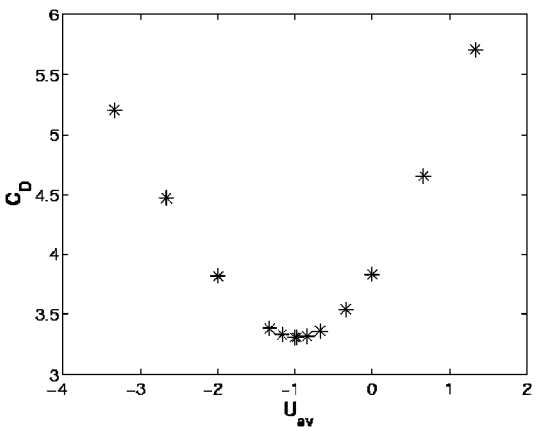

Figure 10. Test 1: drag coefficient for different values of U_{av} (average value of control variable) ($Re = 10$).

DOI: 10.1002/fld

Table I. Test 1: drag coefficients, minimum drag coefficients, average values (optimal) of control function, number of iterations of the optimization procedure and cpu times for different *Re* values; comparison of results for meshes with 2955 (see Figure 3), 4625 and 6467 elements.

Mesh	*Re*	c_D ($\mathbf{u}=\mathbf{0}$)	c_D (opt.)	U_{av} (opt.)	Numbers of iterations	cpu (s)
	5	5.8036	4.7390	−1.7671	44	2295
2955 el.	10	3.8332	3.3066	−0.96676	24	1761
	20	2.6710	2.3323	−0.57954	12	1316
	50	1.7737	1.5185	−0.32516	3	1050
	5	5.8045	4.7401	−1.7679	44	4060
4625 el.	10	3.8337	3.3074	−0.96700	24	2700
	20	2.6712	2.3328	−0.57950	12	2002
	50	1.7731	1.5186	−0.32489	3	1717
	5	5.8046	4.7401	−1.7682	44	6405
6467 el.	10	3.8338	3.3074	−0.96715	24	4446
	20	2.6712	2.3328	−0.57961	12	3406
	50	1.7732	1.5182	−0.32507	4	2935

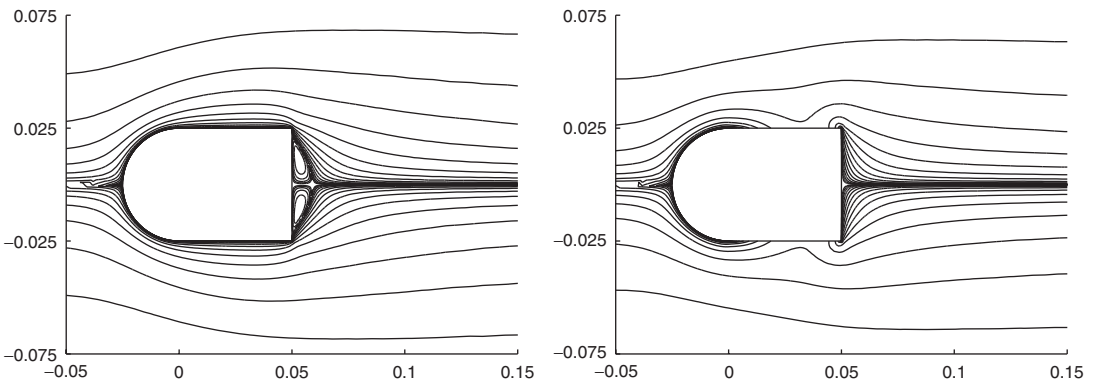

Figure 11. Test 2: streamlines for the initial (left) and optimal (right) state flows ($Re=10$).

procedure. However, let us observe that, as *Re* increases, the computational cost associated with the solution of the Navier–Stokes equations raises: for this reason, the cost of the complete optimization procedure could be great, even if the number of iterations is limited. Moreover, in Table I, we provide a comparison of the results for different triangular meshes with 2955 (see Figure 3), 4625 and 6467 elements. We evidence that, for the *Re* numbers considered, the sensitivity of the results w.r.t. the mesh is limited; this shows that the mesh with 2955 elements (Figure 3) is adequate for the resolution of this optimal control problem.

In Section 3.2, we have anticipated that no stabilization terms for convection have been used for the FE approximation of the Navier–Stokes equations. Numerical tests confirm the validity of this choice, for the meshes and the *Re* numbers considered; for example, by using the mesh with 2955 elements and $Re=50$, the local Reynolds number $Re_K := h/d\ Re$, h being the diameter of the local mesh elements is about $Re_K \lesssim 1$ near the body.

DOI: 10.1002/fld

Table II. Test 2: drag coefficients, minimum drag coefficients, average values (optimal) of control function, number of iterations of the optimization procedure and cpu times for different *Re* values.

Re	c_D ($\mathbf{u}=\mathbf{0}$)	c_D (opt.)	U_{av} (opt.)	Number of iterations	cpu (s)
5	3.9966	3.7802	−0.91485	56	3082
10	2.5624	2.5084	−0.37184	37	2466
20	1.7201	1.6991	−0.18668	21	2060
50	1.0759	1.0577	−0.11335	7	1517

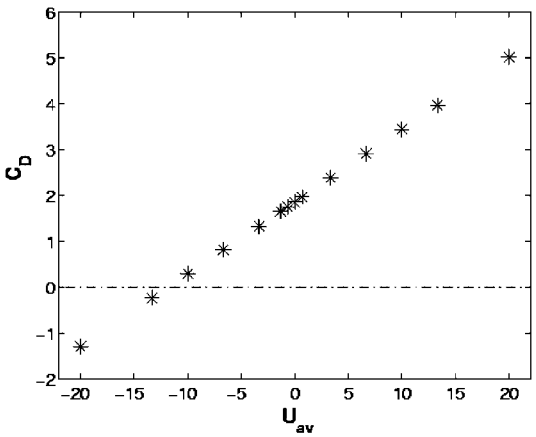

Figure 12. Stokes case: drag coefficient *versus* average value of control variable.

In Remark 3.2, we have discussed a strategy for the reduction of the computational cost of the optimization procedure, for which we initialize the linearized Navier–Stokes state equations with the velocity field computed at previous step of the optimization iterative procedure, instead of using a Stokes solver at each optimization step. Numerical tests, referring to the problem under investigation, outline that cost savings can be reached of about 37 and 25%, for $Re=5$ and 10, respectively (for the mesh with 2955 elements).

Test 2: We consider the case for which $t=d/2=0.05$ (see Figure 2), i.e. the thickness of this body is the half of that considered for Test 1. For the computations, we use a mesh similar to that reported in Figure 3 with 2987 triangular elements (and 1573 vertices).

In Figure 11, we show the streamlines of the initial (left) and optimal (right) flows for $Re=10$, which evidence the effect of the aspiration of the flow across the control boundaries. In Table II, we report the results obtained for this test case, which confirm the considerations made for Test 1; moreover, we evidence that, for this body, the effects of the boundary layer aspiration on the drag coefficient are less evident than for the body of Test 1.

The Stokes case: If we define the drag minimization control problem for the Stokes equations, the drag coefficient does not admit a positive minimum, but tends to $-\infty$; this is due to the linearity in the velocity of the Stokes equations and the drag coefficient.

In Figure 12, we report, referring to Test 1, the drag coefficient (for a prescribed μ) computed for different values of U_{av}, for which the linear dependence of c_D on U_{av} is evidenced.

DOI: 10.1002/fld

5. CONCLUSIONS

In this work, we have studied an optimization control problem for the drag reduction of a 2-D body in relative motion with an incompressible fluid with constant properties. In particular, we have considered as control function the Dirichlet boundary conditions defined on a part of the boundary of the body itself. We have used the Lagrangian functional approach for the resolution of the optimal control problem, together with the Lagrangian multiplier method for the treatment of the Dirichlet boundary conditions. This has allowed a straightforward determination of the Euler–Lagrange system, without introducing lifting terms. We have proved the effectiveness of the procedure on numerical tests by computing the optimal flow for which the drag coefficient is minimum and comparing the results for different *Re* numbers and configurations.

ACKNOWLEDGEMENTS

I would like to acknowledge Prof. A. Quarteroni, Dr F. Nobile and Prof. L. Formaggia for several useful suggestions; also, I acknowledge Prof. A. Veneziani and Dr M. Verani for discussions and for pointing out interesting references. Finally, I acknowledge the referees for the useful comments and suggested improvements.

REFERENCES

1. Becker R. Mesh adaptation for stationary flow control. *Journal of Mathematical Fluid Mechanics* 2001; **3**:317–341.
2. Fourestey G, Moubachir M. Solving inverse problems involving the Navier–Stokes equations discretized by a Lagrange–Galerkin method. *Computer Methods in Applied Mechanics and Engineering* 2005; **194**(6–8):877–906.
3. Fourestey G, Moubachir M. Optimal control of Navier–Stokes equations using Lagrange–Galerkin methods. *INRIA Report RR-4609*, 2002. http://www.inria.fr (15 June 2006).
4. Giles MB, Pierce NA. An introduction to the adjoint approach to design. *Flow, Turbulence and Combustion* 2000; **65**(3–4):393–415.
5. Gunzburger MD. Adjoint equation-based methods for control problems in incompressible, viscous flows. *Flow, Turbulence and Combustion* 2000; **65**:249–272.
6. Gunzburger MD. *Perspectives in Flow Control and Optimization*, *Advances in Design and Control*. SIAM: Philadelphia, 2003.
7. He JL, Glowinski R, Metcalfe R, Nordlander A, Periaux J. Active control and drag optimization for flow past a circular cylinder, I. Oscillatory cylinder rotation. *Journal of Computational Physics* 2000; **163**(1):83–117.
8. Jameson A. CFD for aerodynamics design and optimization: its evolution over the last three decades. *Sixteenth AIAA CFD Conference*, Orlando, FL, U.S.A., 23–26 June 2003, *AIAA Paper 2003-3438* 2003.
9. Mohammadi B, Pironneau O. *Applied Shape Optimization for Fluids*. Clarendon Press: Oxford, 2001.
10. Schäfer M, Turek S, Rannacher R. Evaluation of a CFD benchmark for laminar flows. *Proceedings ENUMATH 1997*, Heidelberg, Germany, 28 September–3 October 1997. World Scientific: Singapore, 1998; 549–563.
11. Agoshkov VI. *Optimal Control Methods and Adjoint Equations in Mathematical Physics Problems*. Institute of Numerical Mathematics, Russian Academy of Science: Moscow, 2003 (in Russian).
12. Lions JL. *Optimal Control of Systems Governed by Partial Differential Equations*. Springer: New York, 1971.
13. Becker R. Mesh adaptation for Dirichlet flow control via Nitsche's method. *Communications in Numerical Methods in Engineering* 2002; **18**:669–680.
14. Gunzburger MD, Manservisi S. The velocity tracking problem for Navier–Stokes flows with boundary control. *SIAM Journal on Control and Optimization* 2000; **39**(2):594–634.
15. Hou LS, Ravindran SS. Numerical approximation of optimal flow control problems by a penality method: error estimates and numerical results. *SIAM Journal on Scientific Computing* 1999; **20**(5):1753–1777.
16. Becker R, Kapp H, Rannacher R. Adaptive finite element methods for optimal control of partial differential equations: basic concepts. *SIAM Journal on Control and Optimization* 2000; **39**(1):113–132.
17. Becker R, Rannacher R. An optimal control approach to a posteriori error estimation in finite element methods. *Acta Numerica* 2001; **10**:1–102.

DOI: 10.1002/fld

18. Dedè L, Quarteroni A. Optimal control and numerical adaptivity for advection–diffusion equations. *M2AN. Mathematical Modelling and Numerical Analysis* 2005; **39**(5):1019–1040.
19. Quarteroni A, Valli A. *Numerical Approximation of Partial Differential Equations*. Springer: Berlin, Heidelberg, 1994.
20. Hou LS, Ravindran SS. A penalized Neumann control approach for solving an optimal Dirichlet control problem for the Navier–Stokes equations. *SIAM Journal on Control and Optimization* 1998; **36**(5):1795–1814.
21. Babuška I, Nobile F, Tempone R. Worst-case scenario analysis for elliptic PDE's with uncertainty. *Proceedings EURODYN 2005*, *Structural Dynamics*. Mill Press: Rotterdam, 2005; 889–894.
22. Maurer H, Mittelmann HD. Optimization techniques for solving elliptic control problems with control and state constraints: Part 1. Boundary control. *Computational Optimization and Applications* 2000; **16**(1):29–55.
23. Gill PE, Murray W, Wright MH. *Practical Optimization*. Academic Press: New York, 1989.
24. Giles MB, Larson MG, Levenstam JM, Süli E. Adaptive error control for finite element approximations of the lift and drag coefficients in viscous flow. *OUCL Numerical Analysis Group Report NA-97/06*, 1997. http://web.comlab.ox.ac.uk/oucl (15 June 2006).
25. Kolmogorov AN, Fomin SV. In *Elements of Theory of Functions and Functional Analysis*, Tikhomirov VM (ed.). Nauka: Moscow, 1989.
26. Girault V, Raviart PA. *Finite Element Methods for Navier–Stokes Equations. Theory and Algorithms*. Springer: Berlin, 1986.
27. Brezzi F, Falk RS. Stability of higher-order Hood–Taylor methods. *SIAM Journal on Numerical Analysis* 1991; **28**:581–590.
28. Taylor C, Hood P. A numerical solution of the Navier–Stokes equations using the finite element technique. *Computers and Fluids* 1973; **1**(1):73–100.
29. Vasil'ev FP. *Methods for Solving the Extremal Problems*. Nauka: Moscow, 1981.
30. Gresho PM, Sani RL. *Incompressible Flow and the Finite Elements Method*. Wiley: New York, 2000.
31. Gunzburger MD. *Finite Element Method for Viscous Incompressible Flows*: *A Guide to Theory*, *Practice and Algorithms*. Academic Press: Boston, 1989.
32. Quartapelle L. *Numerical Solution of the Incompressible Navier–Stokes Equations*. Birkhäuser: Basel, 1993.
33. Quarteroni A, Sacco R, Saleri F. *Numerical Mathematics*. Springer: New York, 2000.
34. FreeFEM.org Web Page. http://www.freefem.org (15 June 2006).

DOI: 10.1002/fld